Capstone Project Report

Relay Networks in the Presence of Co-channel Interference

Submitted to   **:** Dr. Mike MacGregor
                                     Director, Master of Internetworking

Submitted by   **:** Saikalpana Rajendran
Mentor   **:** Mr. Prasanna Herath
Courtesy   **:** Dr. Chintha Tellambura

Master of Internetworking
Department of Electrical and Computer Engineering
University of Alberta

August 2014

Acknowledgement

I take this opportunity to thank Professor Mike MacGregor and Professor Chintha Tellambura for giving me this wonderful opportunity and I am highly indebted to my Mentor Mr. Prasanna Herath for guiding and encouraging me through out the course of this project.

Abstract

To meet the demands of ever increasing wireless traffic, relay networks has been identified as a promising solution. However, they are prone to co-channel interference which arises due to the aggressive reuse of the available spectrum. Therefore, this project investigates the effect of interference on the outage probability of a two-hop channel state information assisted amplify-and-forward relay network. Three networks configurations are considered: (i) relay is subject to interference while the destination is perturbed by additive white Gaussian noise, (ii) relay is under additive white Gaussian noise while destination is subject to interference, (iii) both relay and destination are subject to interference. In all three configurations, interference at each node was assumed to be generated by a Poisson filed of interferers distributed over an annular region. All channels are assumed be subject to exponential path loss and Rayleigh multipath fading. It is shown that the effect of interference can be reduced by having an exclusion zone around the relay and destination. Further, our study indicates that the path loss, which is expected to increase in future generations of wireless systems due to the use of higher frequencies and lower antenna heights, helps to ease the effect of co-channel interference.

Table of Contents

List of Figures

List of Tables

Chapter 1

1.1 Introduction

Wireless technologies have undergone a tremendous growth recently. Cisco forecasts the number of mobile devices to exceed the global population in 2014 [1]. The mobile data traffic is expected to reach 16 Exabyte per month in 2018 [1]. To meet these demands, future generations of wireless systems must be more reliable, more power efficient (greener), and capable of providing higher data rates over a large coverage area. To this end, relay communication has been identified as one of the promising solution. The idea here is to use intermediate nodes to assist the source to destination communication by relaying signals from one hop to the other. Due to shorter hops, a relay network achieves broader coverage and enhanced throughput [2]. It can also provide network connectivity to locations where the traditional single-hop architecture may not be able to reach. The battery life of mobile devices may be prolonged due to lower power requirements. Furthermore, relays can reduce the infrastructure cost and total power consumption of wireless systems. Due to those immense benefits, relay networks are currently being studied for next generation wireless standards such as Long Term Evolution-Advanced (LTE-A).

1.2 Motivation

The performance improvements achieved via relays can be greatly degraded by co-channel interference. Co-channel interference, which arises due to the aggressive reuse of available frequency spectrum, is a fundamental limiting factor in wireless networks. Therefore this project aims to characterize the performance of relay networks in the presence of interference, which is essential for system design improvements. The study will focus on two-hop relay networks (Figure 1.1) and interference at relay and/or destination will be considered. Outage probability, which is an important quality of service measure in any wireless communications system, will be used as the performance metric.

In a two-hop relay network, a radio signal is transmitted from the source to a destination via a Relay Station (RS). Depending on the operation performed at the relay, relay communication systems can be divided into two main categories, namely, amplify-and-forward (AF) relaying and decode-and-forward (DF) relaying. Due to the simplicity of its operation, in this study, AF relaying is considered.

In AF relaying, the received signal at the relay is amplified and forwarded to the destination.
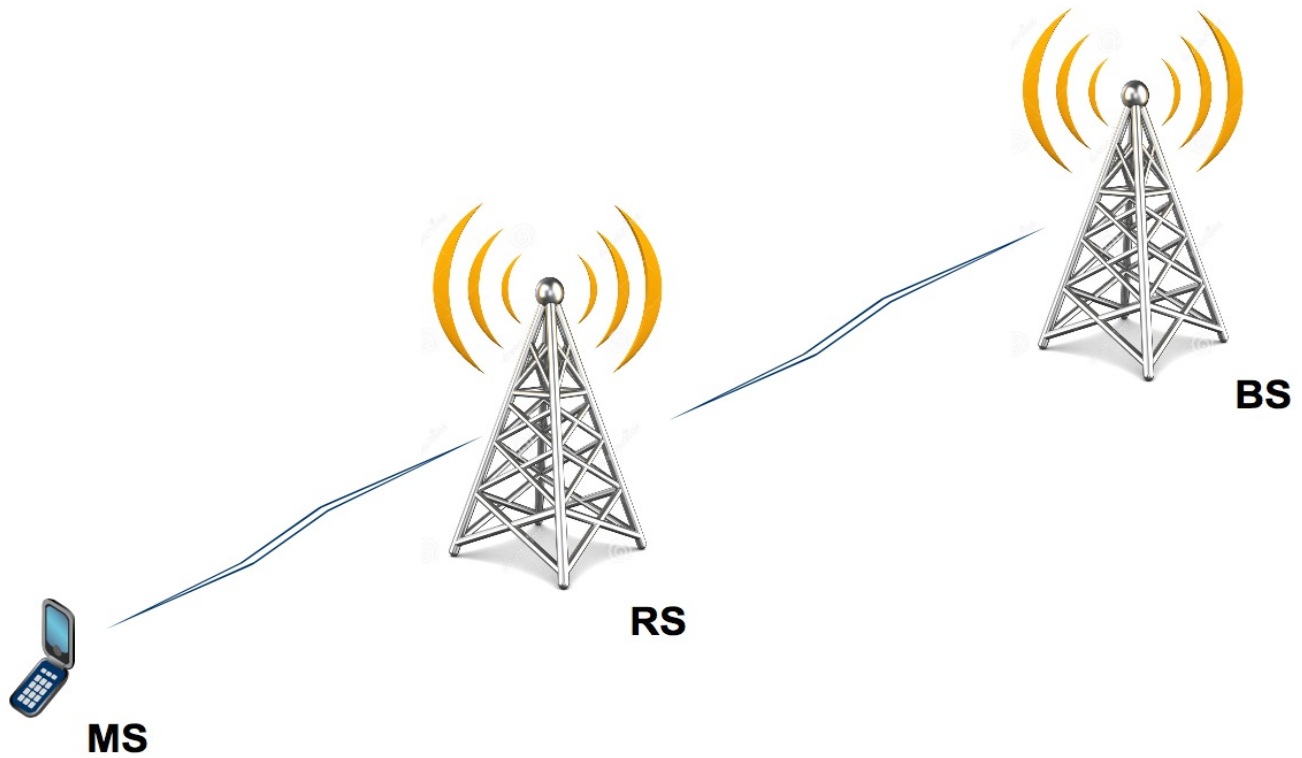
In addition to co-cannel interference, impairments inherited in the wireless radio links also affect the performance of relay networks. In this study two such impairments are considered namely, multipath fading and path loss.

1.3 Background Theory

Co-channel interference, path loss, multipath fading, and shadowing are among the performance limiting factors in wireless communications. Co-channel interference arises due to the aggressive reuse of the frequency spectrum. Path loss reduces the received signal strength with the transmitter-receiver distance. Shadowing and multipath fading creates random fluctuations in the received signal strength. This section details these phenomenon and the associated concepts.

1.3.1 Co-channel interference

Frequency reuse plays a vital role in Cellular communication systems. Any cellular system aims at establishing radio communication between a mobile station (MS) and a grid of base stations (BSs) [2]. This grid of base stations is deployed on the coverage area, which is divided into small hexagonal cells (Refer Figure 1.3). The efficiency of a cellular system depends on the size of the cell, the ability of the link between BS and MS to withstand interference and the traffic in the communication medium [2].

Frequency Reuse and the Cellular Concept

Cellular communication systems that are based on Time Division Multiple Access (TDMA) and Frequency Division Multiple Access (FDMA) are based on frequency reuse, where users belongs to geographically separated cells simultaneously use the same carrier frequency [2]. The cellular layout of macro-cellular systems is often described by a uniform grid of regular hexagons. In practice cells are not regular hexagons, but are distorted and overlapped areas [2]. Hexagons are mainly used as it closely approximates a circle and offers a wide range of tessellating reuse cluster sizes [1, 2]. With the hexagonal cell structure, a tessellating reuse cluster of size N can be constructed if

$$N = i^2 + i\,j + j^2,$$

where i and j are non-negative integers, and $i \geq j$. Therefore, the allowable cluster sizes are $N = 1, 3, 4, 7, 9, 12$ ... Examples of 3- and a 7-cell reuse clusters are shown in Figure 1.2.

Figure 1.2: 3-cell and 7-cell reuse clusters [2]

In cellular systems, each cluster is allocated a group of frequencies distributed among individual

3

hexagonal cells and the cluster is replicated through out the coverage area along with the allocated frequency channels. The coverage area with replicated 7-cell reuse cluster is shown in the Figure 1.3. Cells with the same letter are assigned the same carrier frequencies. With this configuration, after a specific geographical distance the same frequency is assigned to another cell (Refer Figure 1.3) [2]. This distance is referred as the co-channel reuse distance. For a cellular system with cluster size of N, co-channel reuse distance R_d is given by

$$R_d = R \sqrt{3N},$$

where R is the radius of a hexagonal cell. If S is the total number of duplex channels available for use and if there are N cells in a cluster, the number of channels allocated for each cell is given by

$$k = \frac{S}{N}.$$

If M is the number of clusters in the system, the total number of users the communication system can serve is given by

$$C = MS.$$
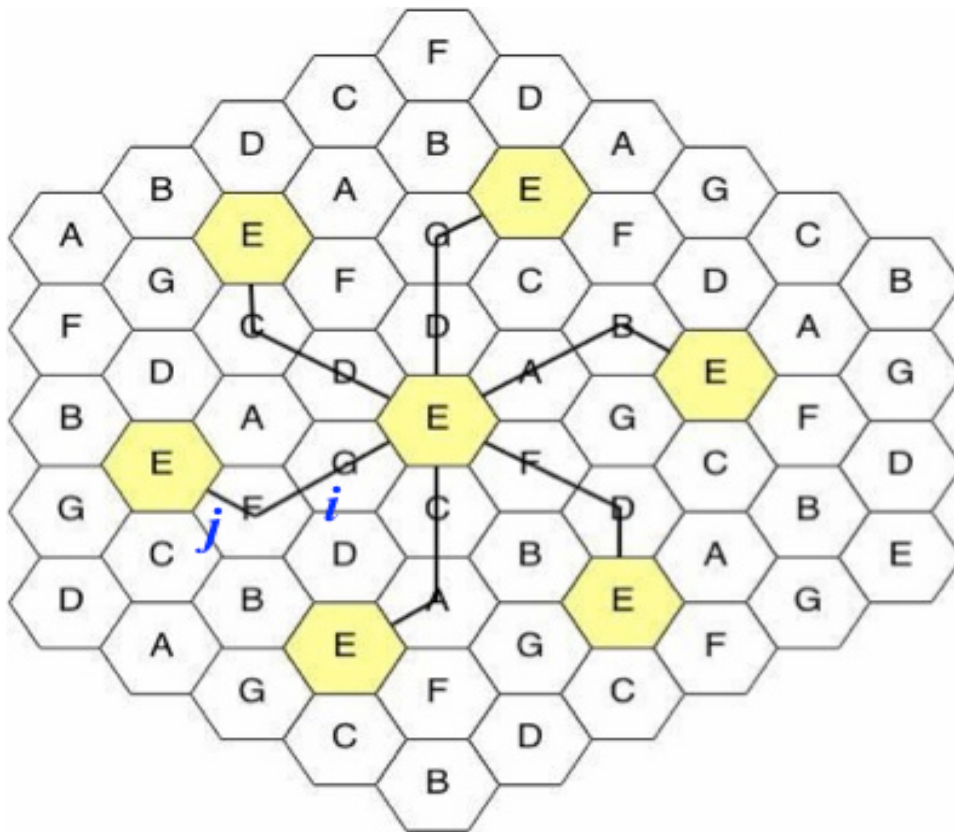
Figure 1.3 Frequency re-use concept [2]

When the cell radius is small, a given area can be fitted with a larger number of clusters, thus higher the number of simultaneous users a cellular network can serve [2]. In other terms, it improves the spectral efficiency of the system [2]. However, smaller cells reduce the reuse distance that can detrimentally affect the performance of the system due to increased level of co-channel interference.

1.3.2 Path loss

The effect of path loss, shadowing and multipath fading on the normalized received power in a wireless channel is shown in Figure 1.4. Path loss exponential decays the received signal power with the transmitter-receiver distance. The variation in signal power occurs over a very large distance of 100 m to 1000 m. Path loss highly depends on the propagation medium [2, 11].
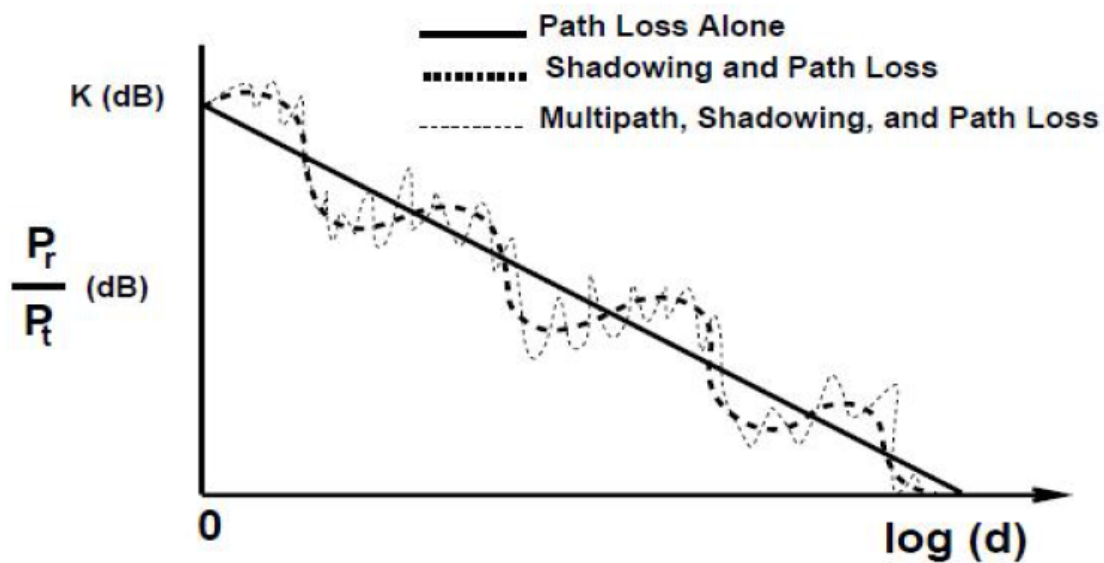
Figure 1.4: Path loss, Shadowing and Multipath fading [10]

1.3.2.1 Path-loss models

In a wireless environment, path loss can be modeled using empirical models for a specific geographical area for a given transmitter-receiver distance and frequency. These empirical models can be used for analyzing the performance of wireless communication systems [10]. Some empirical path loss models are listed below [10].

- Okumura model
- Hata model
- Piecewise linear model

However, for general analysis of various system designs, a simple model named 'the simplified path loss model' is used instead of complex empirical models [10].

Simplified Path loss model

In the simplified path loss model, the received power is given by

$$P_r = P_t K \left[\frac{d_0}{d}\right]^\alpha,$$

where, P_r is the received power and P_t is the transmitted power and K is a constant that depends on the antenna characteristics and the attenuation caused by the channel. α represents path loss component and d_0 is the reference distance for antenna far-field which is assumed to be 1-10 m for indoors and 10-100 m for outdoors [10]. Typical path-loss factor values are given below (Refer Table 1.1). Converting to dB scale

$$P_{r(dBm)} = P_{t(dBm)} + K\,(dB) - 10\alpha \log_{10} \left[\frac{d}{d_0}\right].$$

Environment	α Range
Urban macrocells	3.7-6.5
Urban microcells	2.7-3.5
Office building (same floor)	1.6-3.5
Office building (multiple floors)	2-6
Store	1.8-2.2
Factory	1.6-3.3
Home	3

Table 1.1 Typical path-loss factors [10]

1.3.3 Fading

Fading is the deviation of the attenuation of a radio signal arising due to multipath propagation in a wireless communication medium (Refer Figure 1.4). Fading is modeled as a random process since it can vary with time and geographical position. Fading can be classified into two types namely, fast fading and slow fading [2, 11]. The rate at which the channel imposes magnitude and phase changes on the radio signal determines the type of fading the signal undergoes.

1.3.3.1 Slow fading

Slow fading occurs when the coherent time of the channel is much greater than the delay factor of the channel. The minimum time taken by the propagation channel to impose changes to the magnitude by which the magnitude reaches a value completely uncorrelated to its previous value is called the coherent time of the channel. Shadowing is produced by relatively large objects such as buildings and mountains [2, 11]. In such a scenario, the magnitude and phase changes are imposed on the radio signal by the propagation channel is almost constant over a particular period of time (Refer Figure 1.4). The statistical model that represents slow fading is called the log normal distribution model [2].

Log normal distribution model

The most common assumption for slow fading is lognormal distribution. This model has been confirmed empirically to accurately model the variation in received power in both outdoor and indoor radio propagation environments. Under this fading model the Probability Density Function (PDF) of the squared envelope is given by

$$f(x) = \frac{1}{x\sigma_{dB}\,\xi\sqrt{2\pi}}\exp\left(-\frac{(10\,log_{10}\,x - \mu_{dB})^2}{2\sigma_{dB}{}^2}\right), x > 0,$$

where, $\xi = \frac{\ln 10}{10}$. μ_{dB} and σ_{dB} represent the mean and the variance of fading power in dB.

1.3.3.2 Fast fading

Fast fading is caused by multipath propagation and it creates rapid fluctuations in the signal strength (Refer Figure 1.4). Unlike slow fading, fast fading arises when the coherent time of the channel is larger than the delay constraint of the channel. Several statistical models have been proposed to model slow fading. Some of the most common models are [2] listed below.

- Rayleigh fading
- Rician fading
- Nakagami$-m$ fading

Rayleigh fading

Rayleigh distribution model represents the multipath fading with no direct line-of-sight (LOS) whose channel impulse response can be represented using a Gaussian process with phase uniformly distributed between 0 and 2π. A signal propagating through such a channel undergoes random changes in its magnitude. These changes in magnitude cause the signal to fade rapidly. Under this model, the probability density function (PDF) of the envelope of the signal can be represented by [2]

$$f_{\alpha(\alpha)} = \frac{\alpha}{\sigma^2} \exp\left(-\frac{\alpha^2}{2\sigma^2}\right), \alpha \geq 0,$$

where σ^2 is the variance of in-phase and quadrature phase components. Then the PDF of the signal to noise ratio (SNR) is given by

$$f_{\gamma(\gamma)} = \frac{1}{\overline{\gamma}} \exp\left(-\frac{\gamma}{\overline{\gamma}}\right), \gamma \geq 0,$$

where $\overline{\gamma}$ is the average SNR.

Rician fading

Rician distribution model represents signal fading where the channel contains one strong/direct line of sight (LoS) component with many reflected or scattered components. The PDF of the Rician fading envelope is given by [2]

$$f\alpha(\alpha) = \left(\frac{\alpha}{\sigma^2}\right)\exp\left(-\frac{\alpha^2 + A^2}{2\sigma^2}\right)I_0\left(\frac{a}{\sigma^2}\right), \alpha \geq 0,$$

where σ^2 is the variance of in-phase and quadrature phase components and $I_0(.)$ is the zeroth order of modified Bessel function of the first kind. The Rician distribution is characterized by Rician factor K, which is defined as the ratio of the specular power A^2 to scattered power $2\sigma^2$. Therefore,

$$K = \left(\frac{A^2}{s\sigma^2}\right).$$

- When $K = 0$, the channel exhibits Rayleigh fading [2].
- When $K \rightarrow \infty$, the channel does not exhibit any fading [2].

The PDF of signal to noise ratio (SNR) under Rician fading is given by [11]

$$f_{\gamma(\gamma)} = \frac{K+1}{\overline{\gamma}}\exp\left(-K - \frac{(K+1)\gamma}{\overline{\gamma}}\right)I_0\left(\frac{2\sqrt{K(K+1)\gamma}}{\overline{\gamma}}\right), \gamma \geq 0,$$

where, $\overline{\gamma}$ is the average SNR.

Nakagami$-m$ fading

Nakagami$-m$ fading model can be used to model multipath fading with a wide range of fading severities. This model can be used in channels where the fading conditions are more or less severe than Rayleigh fading [2]. The PDF of the Nakagami$-m$ fading envelope is given by [2]

$$p_{\alpha(x)} = \frac{2m^m x^{(2m-1)}}{\Gamma(m)\Omega^m}exp\left(\frac{mx^2}{\Omega_p}\right), m \geq \frac{1}{2}.$$

- When m $= 1$, Nakagami distribution becomes Rayleigh distribution.
- When m $= \frac{1}{2}$, Nakagami distribution becomes one-sided Gaussian distribution.
- When m $\rightarrow \infty$, no fading is experienced.

Rician distribution can also be closely approximated by Nakagami$-m$ fading model by using following two identities

$$K = \frac{\sqrt{m^2 - m}}{m - \sqrt{m^2 - m}}, m > 1.$$

$$m = \frac{(K + 1)^2}{2K + 1}.$$

1.4 Relay Networks

In wireless communication, the distance between the transmitter and the receiver plays a major role in path-loss and fading effects on the radio signal. This distance can be broken into shorter hops using intermediate nodes called relays. A dual-hop communication system involving a relay is shown below.

Figure 1.5 A dual-hop relay communication system
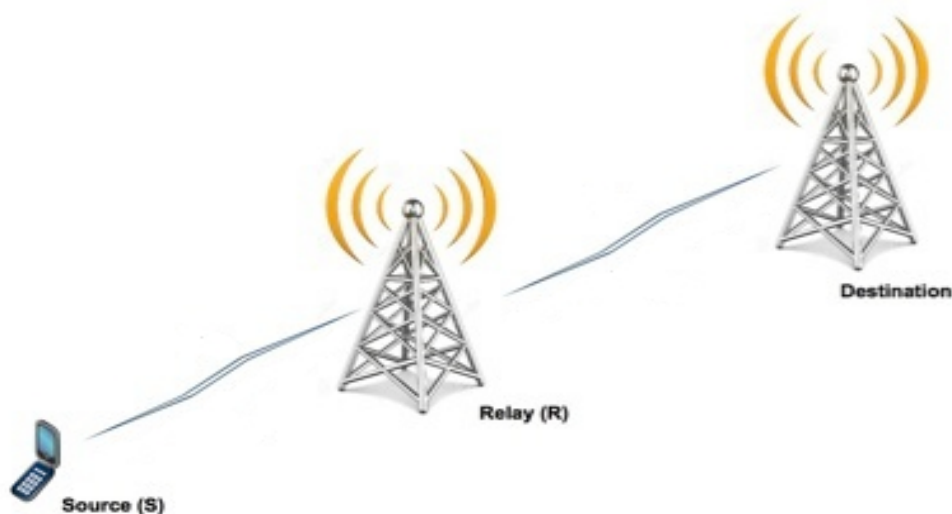
Relays help in improving the overall throughput of the communication system by limiting the effects of path-loss and fading on the radio signal and thereby increasing network coverage and reduces power requirement. Based on the relaying operation performed at the relay, relays can be mainly categorized into two, namely

1. Amplify-and-Forward Relays
2. Decode-and-Forward Relays

1.4.1 Amplify-and-Forward

In Amplify-and-Forward (AF) relaying, also referred to as non-regenerative relaying, the relay amplifies the received signal and forwards it to the destination. Consider a two-hop relay network (Refer Figure 1.6) where y_{SR} is the signal received by the relay (R) from the source (S). Mathematically, y_{SR} can be given as [12, 13]

$$y_{SR} = \sqrt{P_S}\, r_{SR}^{-\frac{\alpha}{2}} h_{SR} x + n_{SR},$$

where, x represents the transmitted signal from the source and h_{SR} is the channel gain co-efficient of the $S-R$ channel. P_S is the transmit power at the source and n_{SR} is the Additive white Gaussian Noise (AWGN) of the source to relay channel with variance N_{SR}.

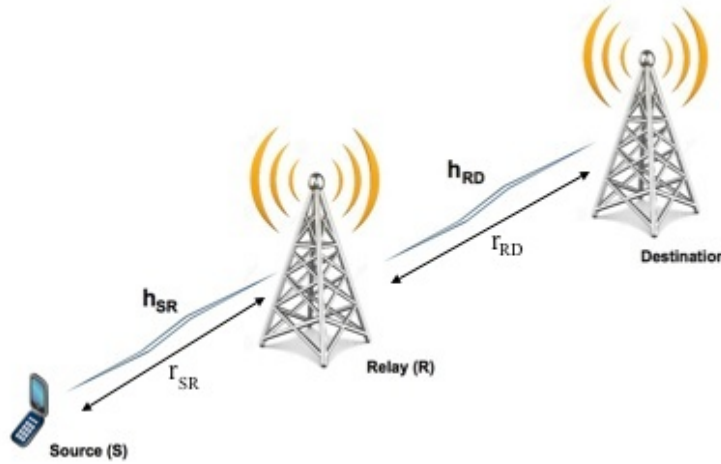

Figure 1.6 Amplify and forward

During the second phase, the relay amplifies the signal received from the source by gain G. Therefore; the signal transmitted by the relay is given by

$$x_R = G\, y_{SR}.$$

The received signal at the destination is given by

$$y_{RD} = h_{RD}\, G\, y_{SR} + n_{RD,}$$

where h_{RD} is the $R-D$ channel coefficient and n_{RD} is the AWGN at the destination.

1.4.1.1 CSI Assisted Relays

CSI Assisted relays are different from the other relays in the method of channel gain selection. The Channel gain G is selected considering the channel conditions between the source and relay [14]. Sometimes the channel noise is also considered and hence it is called as channel-noise-assisted amplify and forward relaying [15]. The gain of a CSI assisted relay can be expressed as

$$G = \sqrt{\frac{P_R \, r_{RD}^{-\alpha}}{P_S \, r_{SR}^{-\alpha} |h_{SR}|^2 + N_{SR}}},$$

where, E_R is the average energy per symbol transmitted at the relay. The end-to-end signal-to-noise ratio (SNR) can be given by [12],

$$\gamma_R = \frac{\gamma_{SR}\gamma_{RD}}{\gamma_{SR} + \gamma_{RD} + 1}.$$

When the channel noise is ignored, the channel gain G becomes

$$G = \sqrt{\frac{P_R \, r_{RD}^{-\alpha}}{P_S \, r_{SR}^{-\alpha} |h_{SR}|^2}}.$$

And the end-to-end SNR can be given by

$$\gamma_R = \frac{\gamma_{SR}\gamma_{RD}}{\gamma_{SR} + \gamma_{RD}}.$$

Implementation of CSI assisted relays is difficult due to the need of continuous monitoring of channel fading amplitudes [16].

1.4.1.2 Fixed gain relays

In fixed gain relays, the received signal at the relay is amplified by a fixed gain value irrespective of the fading amplitude of the signal. When P_R is the average energy per symbol

transmitted at the relay and N_{SR} is the AWGN in the source to relay channel, the fixed gain can be represented by the following expression

$$F_G = \sqrt{\frac{P_R \, r_{RD}^{-\alpha}}{C N_{SR}}}.$$

And the end-to-end SNR of fixed gain relays can be expressed as [16],

$$\gamma_R = \frac{\gamma_{SR}\gamma_{RD}}{C + \gamma_{RD}},$$

where, C is a constant that varies when the fixed gain value F_G is to be varied.

1.4.2 Decode and Forward

In Decode-and-Forward relaying [12], there are two phases involved. In the first phase, the relay decodes the entire signal received from the transmitter. In the second phase, the relay re-encodes the signal before forwarding it to the destination. Decode-and-Forward helps to reduce noise at the relay but there are possibilities of forwarding an erroneous signal to the destination [18]. Also, this type of relaying requires more power when compared with Amplify-and-Forward for decoding and encoding processes [17].

1.5 Spatial Point Processes for Modeling of Cellular Network

To meet the exponential growth in the demand of wireless traffic, day by day, different types of BSs are added to the existing macro cellular networks. In these networks, macro BSs are expected to provide the umbrella coverage while the deployment of small BSs such as pico-BSs, femto access points (femto-APs), and relays are expected to provide coverage to dead spots and capacity demanding hotspots. The moving towards heterogeneity has introduced additional randomness to the location of BSs in wireless systems. It has been shown that spatial distribution of BSs of these emerging class of wireless systems can be appropriately modeled by using Point processes [3, 4, 5, 6,7]. To this end,

Poisson point process (PPP) [8, 9] has extensively been used. In this study, homogeneous PPP [8, 9] over 2-dimensional space (Refer Figure 1.7) is used to model the locations of interferers in two-hop relay networks.

1.5.1 Homogeneous Poisson Point Process

In a homogeneous Poisson point processes over 2-dimensional plane, the number of nodes $N(A)$ reside within an area A that is Poisson distributed. $N(A)$ nodes are uniformly distributed over A.
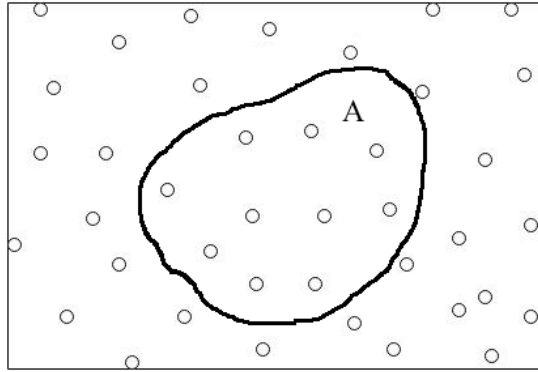
Figure 1.7 Homogeneous Poisson process over a 2-D plane

If the intensity (density) of the PPP is λ, the probability mass function (PMF) of $N(A)$ is given by [Kingman Book]

$$P(N(A) = x) = \frac{(\lambda A)^x e^{-\lambda A}}{x!} , x = 0,1,2 \dots$$

In this study, interferers are assumed to be distributed over an annular region around the relay and/or destination with constant density (Refer Figure 1.8)

For an annular region with inner radius R_g and outer radius R_e, the number of interferers is Poisson distributed and its PMF is given by [Kingman Book]

$$P(N(A) = x) = \frac{\left(\lambda \pi (R_e{}^2 - R_g{}^2)\right)^x e^{-\left(\lambda \pi (R_e{}^2 - R_g{}^2)\right)}}{x!} , x = 0,1,2 \dots$$
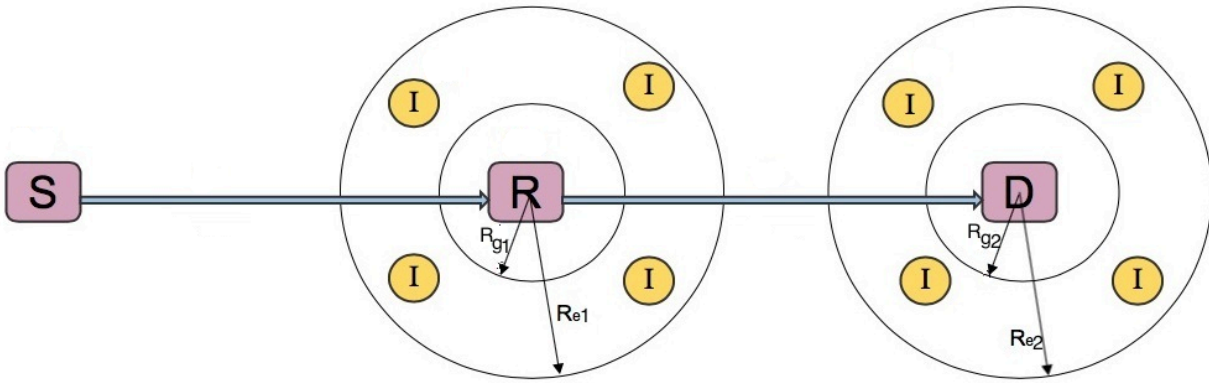
With this configuration, probability distribution function (PDF) of the distance between the receiving node (either relay or destination) located at the center of an annular region and a typical interferer is given by

$$f_R(r) = \frac{2\,r}{(R_e{}^2 - R_g{}^2)}\ , R_g < r < R_e.$$

The angular position of interferers is uniformly distributed over $[0, 2\,\pi]$.

Simulation of a homogeneous PPP over an annular region is discussed in the Appendix.

Chapter 2

Relay Communication with Poisson Field of Interferers

In this chapter the outage probability of the downlink of a two-hop relay network is investigated. The source, which is assumed to be a macro-BS, is located in a deeply shadowed environment, thus there is no direct link with the destination. All the nodes are half duplex and therefore cannot transmit and receive simultaneously. The communication is carried out in two orthogonal phases. In the first phase of communication source transmits to the relay. The amplify-and-forward (AF) relaying is assumed as it minimizes the complexity of the relaying process. Therefore, during the second phase, relay amplifies the received signal corrupted by additive white Gaussian noise or interference and forwards to the destination. All the radio channels are assumed to be subject to exponential path loss with path loss exponent $\propto$ and Rayleigh fading. We consider following three cases for the effect of interference on the network.

- Relay is subject to interference while the destination is perturbed by additive white Gaussian noise (AWGN)
- Relay is under AWGN while destination is subject to interference
- Both relay and destination are subject to interference

The outage probabilities of these networks were investigated using computer simulations written in Matlab®. A description on the steps followed to simulate the Poisson field of interferes is given in Appendix I.

2.1 Two Hop Relay Networks with Interference at the Relay

In this section, the relay is assumed to be under the influence of Poisson filed of interferes distributed over an annular region defined by inner radius R_g and outer radius R_e (Refer Figure: 2.1). In modern cellular networks with multiple tiers of BSs, interference from small BSs such as pico-BS, femto-APs can be received at a relay. These interferers are represented by the Poisson field.
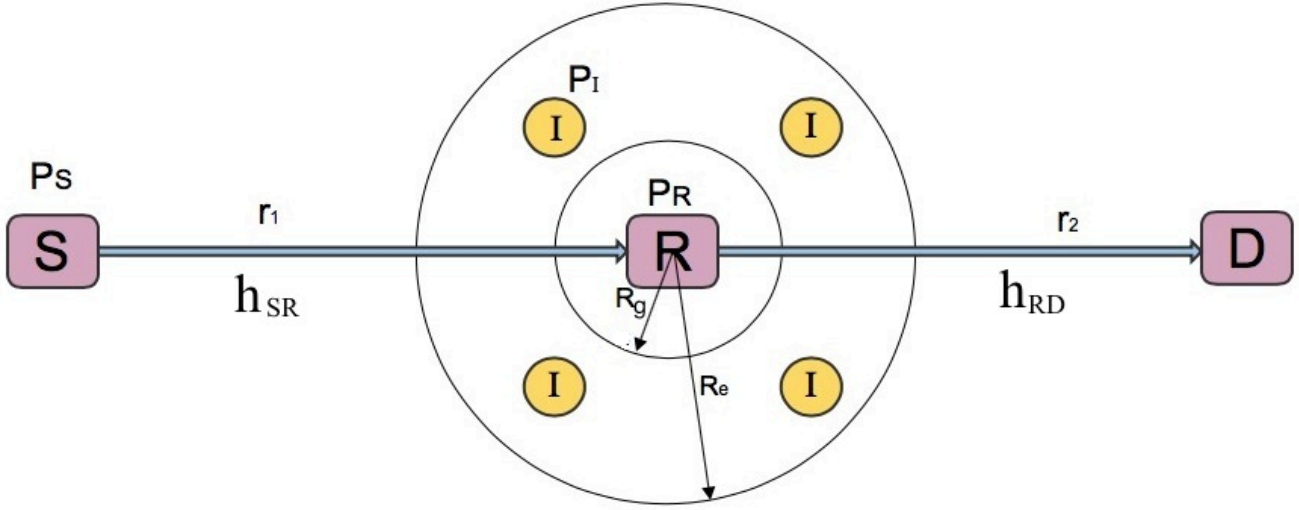
Figure 2.1: Two-hop relay network with Interference at the Relay

The received signal at the relay after the first phase of communication can be represented as

$$y_R = \sqrt{P_S}\, r_1^{-\left(\frac{\alpha}{2}\right)} h_{SR}\, s_0 + \sum_{x \in \phi} \sqrt{P_I}\, ||x||^{-\alpha} h_x,$$

where ϕ represents the Poisson field of interferers and s_0 is the transmitted signal with $E[S_0] = 1$ where $E[.]$ is the expectation operation. Transmitted power at S and interfering nodes are given by P_S and P_I, respectively. The Euclidean distance between the interferers located at $x \in \phi$ and R is denoted by $||x||$. h_{SR} and h_x are the channel gain coefficients of $S - R$ link and the link between interferer located at $x \in \phi$ and the relay. The distances between $S - R$ and $R - D$ channels are represented by r_1 and r_2, respectively. Since CSI assisted variable gain relaying is assumed, the relay amplifies the receive signal by the gain

$$G = \sqrt{\frac{P_R}{P_S r_1^{-\left(\frac{\alpha}{2}\right)} |h_{SR}|^2}}.$$

In the calculation of the relay gain, it is assumed that the relay have no knowledge of the CSI of interfering signals and their transmit powers. This will be the case in practice as measuring the CSI of

each channel is very difficult in large wireless networks. The received signal at the destination can be written as

$$y_D = r_2^{-\frac{\alpha}{2}} h_{RD} G \, y_R + n_D,$$

where n_D is the AWGN at the destination with variance N_0. The end-to-end signal-to-interference plus noise ratio (SINR) at D after two phases of communication can be derived as,

$$\gamma_{eq} = \frac{\left(\dfrac{P_S r_1^{-\alpha} |h_{SR}|^2}{\sum_{x \epsilon \phi} P_I r_x^{-\alpha} \, |h_x|^2}\right) \times \left(\dfrac{P_R r_2^{-\alpha} |h_{RD}|^2}{N_0}\right)}{\left(\dfrac{P_S r_1^{-\alpha} |h_{SR}|^2}{\sum_{x \epsilon \phi} P_I r_x^{-\alpha} \, |h_x|^2}\right) + \left(\dfrac{P_R r_2^{-\alpha} |h_{RD}|^2}{N_0}\right)}$$

$$\gamma_{eq} = \frac{\gamma_{SR} \gamma_{RD}}{\gamma_{SR} + \gamma_{RD}}.$$

where $\quad ||x|| = r_x, \quad \gamma_{SR} = \frac{P_S r_1^{-\alpha} |h_{SR}|^2}{\sum_{x \epsilon \phi} P_I r_x^{-\alpha} \, |h_x|^2}$ and $\gamma_{RD} = \frac{P_R r_2^{-\alpha} |h_{RD}|^2}{N_0}$ are the instantaneous signal-to-interference ratio (SIR) of the S-R channel and R-D channels.

2.1.1 Outage Probability Analysis

The outage P_{out} probability is an important quality of service (QoS) measure in any communication networks. It is defined as the probability that the instantaneous end-to-end SINR falls below a give threshold γ_{th}. Mathematically P_{out} can be written as

$$P_{out} = \mathbf{Pr}\,(\gamma_{eq} < \gamma_{th})$$

$$P_{out} = \boldsymbol{Pr}\,\left(\frac{\gamma_{SR} \gamma_{RD}}{\gamma_{SR} + \gamma_{RD}} < \gamma_{th}\right).$$

2.1.2 Numerical Results and Discussion

This section presents the outage probability of a two-hop relay networks with interference at the relay for various networks configurations.
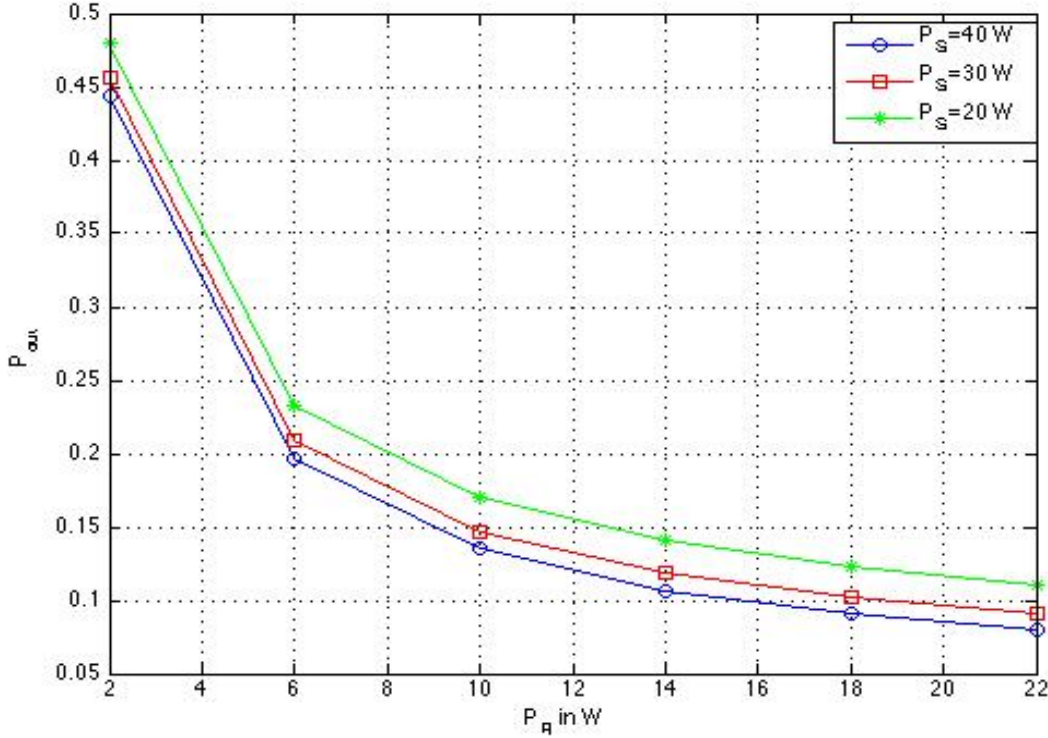

Figure 2.2: Variation of Outage probability with relay power P_R for various values of source powers P_S, when $\alpha = 3, R_g = 200m, \lambda = 1 \times 10^{-6}, r_1 = 200m, r_2 = 100m$.

Figure 2.2 shows the variation of the outage probability with the transmit power at the relay P_R for different values of source transmit power. Initially as P_R increases, the outage probability drops rapidly (lower the outage probability, better the networks performance). However, as P_R increases further, the rate of the drop reduces. For example, when $P_S = 30\ W$, increase of P_R from $2W$ to $10\ W$ drops the outage probability from 0.45 to 0.15. However, further increase of P_R from $10\ W$ to $20\ W$ only drops the outage probability from 0.15 to 0.1. This is because, in relay networks, the end-to-end performance is dominated by the performance of the worst hop. Therefore, when P_R is smaller, the weak $S - D$ hop dominates the performance. Then a small increase in relay power improves the network performance considerably. However, increase in P_R also increases the relay gain. Higher relay gain detrimentally

affects the network performance as at the relay not only the signal it receives but also the interference gets amplified. Results also shows that a marginal improvement in the outage performance can be achieved by increasing the source transmit power.
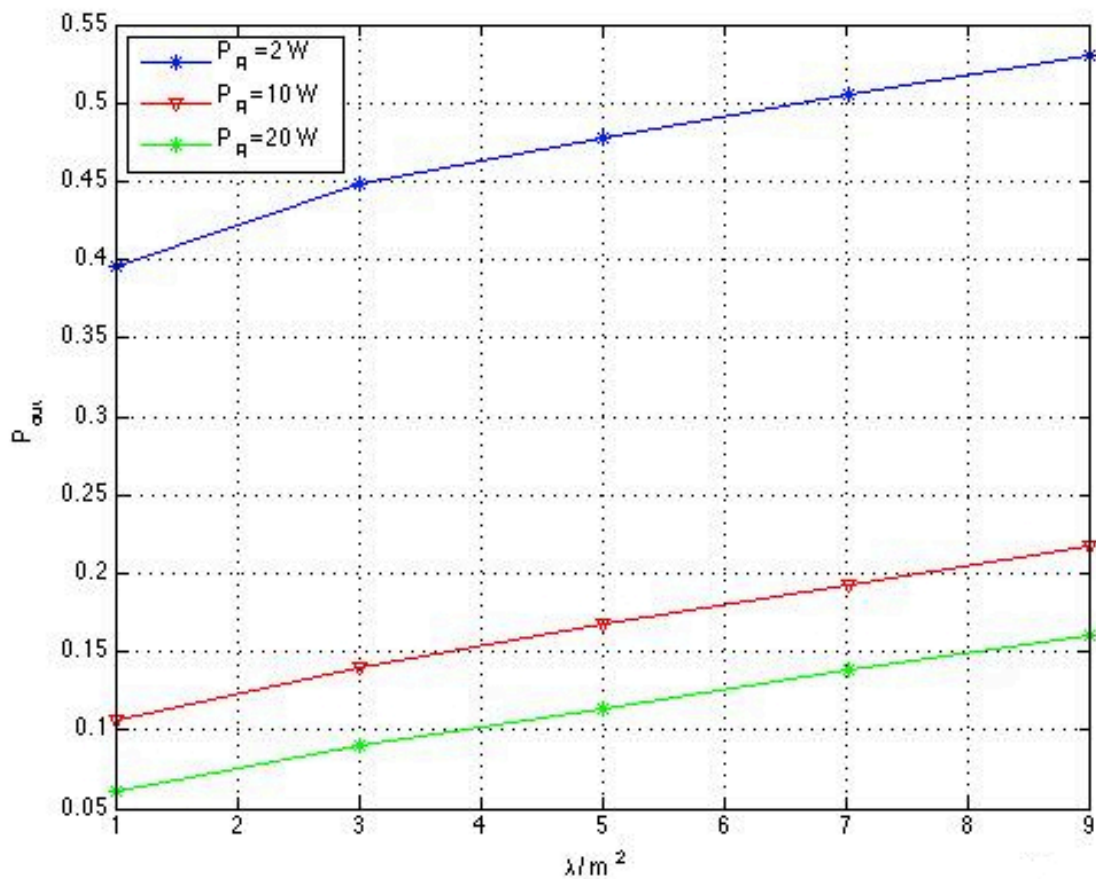
Figure 2.3: Variation of Outage probability with intensity lambda (λ) for various values of relay powers P_R when $\alpha = 3, R_g = 200m, r_1 = 200m, r_2 = 100m, Ps = 30\,W$.

Figure 2.3 shows the variation of the outage probability with intensity of interferers λ for the various values of relay transmit powers P_R. Results show that the outage probability of the networks increases a λ increases. When λ increases the total number of interferers residing in the annular region increases. This increases the total received interference power at the relay. Therefore, the reliability of the network reduces. Results also shows that the outage probability can be reduced by increasing the

relay transmit power. The outage probability sharply drops when P_R increases initially. However, the drop in outage probability due to further increase of P_R is marginal. For example, at $\lambda = 5$ BSs per km^2, the outage probability drops from 0.48 to 0.17 when the P_R increases from 2 W to 10 W. However, further increase of P_R by 10 W only drops the outage probability to 0.12. This is because in AF relaying, both signal and interference get amplified and higher P_R corresponds to increased relaying gain.
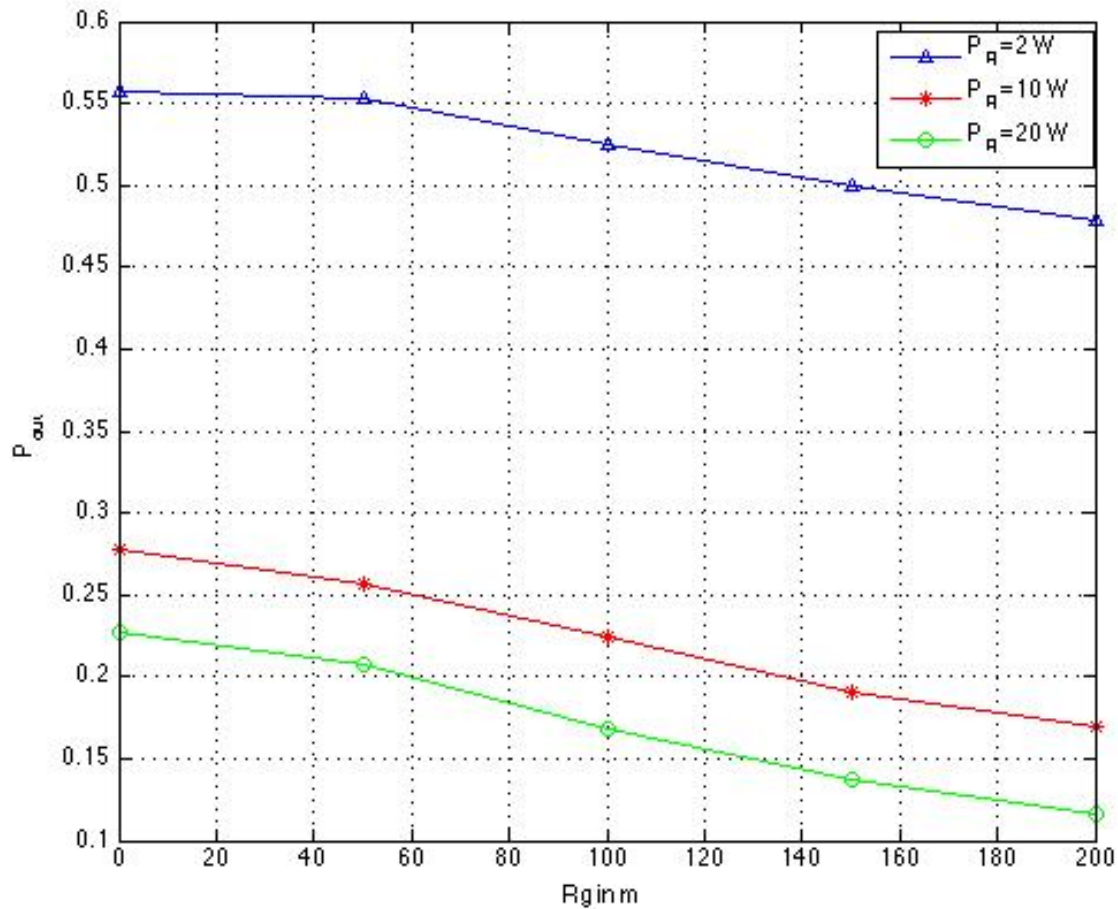

Figure 2.4: Variation of Outage probability P_{out} with exclusion zone radius R_g for various values of relay power P_R when $\alpha = 3, P_S = 30\,W, \lambda = 1 \times 10^{-6}, r_1 = 200m, r_2 = 100m.$

21

The variation of the outage probability with Rg is shown in Figure 2.4 for various values of relay transmit powers P_R. R_g defines an exclusion zone for interferers around the relay. Figure shows that the performance of the network can be considerably increased by having a considerable exclusions zone around the relay. For example, at 20 W of relay power, an exclusion zone of 200 m reduces the outage probability from 0.22 to 0.12. This is because the path loss exponentially decays the interference power with its distance to the receiver. Therefore, the total interference at the relay is dominated by the few interferers located in the vicinity of the relay. Defining an exclusion zone around the relay prevents these highly influential interferers from sharing the resource blocks (time-frequency channel) with the $S - R$ transmission. Because of this a decrease in the outage probability can be observed. Figure also indicates that, when R_g increases, the rate at which the outage probability drops with R_g decreases. Further, having large exclusions zone around relays can reduce the area spectral efficiency and the capacity of the networks. Therefore, in conclusion, having a considerable exclusion zone is important to maintain a lower outage probability. However, a large value of Rg is not required.

2.2 Two Hop Relay Networks with Interference at the Destination

In this section a two hop relay network is considered when the relay-destination transmission is corrupted by interference from a Poisson field of interferes distributed over an annular region. The source-relay communication is assumed to be perturbed by AWGN. Destination is assumed to be interference-limited thus AWGN is not considered. Similar to in section 2.1, CSI assisted AF relaying is considered.

In this network, after the first phase of communication, the received signal at the relay can be written as

$$y_R = \sqrt{P_S}\, r_1^{-\left(\frac{\alpha}{2}\right)} h_{SR}\, s_0 + n_R,$$

where n_R is the AWGN at the relay and h_{SR} and h_{RD} are the channel gains of the source to relay and relay to destination channels respectively. In the second phase of communication, relay amplifies the received signal by gain G and forwards to the destination. This can be mathematically expressed as

$$y_D = \sqrt{P_R}\, r_2^{-\left(\frac{\alpha}{2}\right)} h_{RD}\, G y_R + \sum_{x \in \varphi} \sqrt{P_I}\, ||x||^{-\alpha}\, h_x.$$
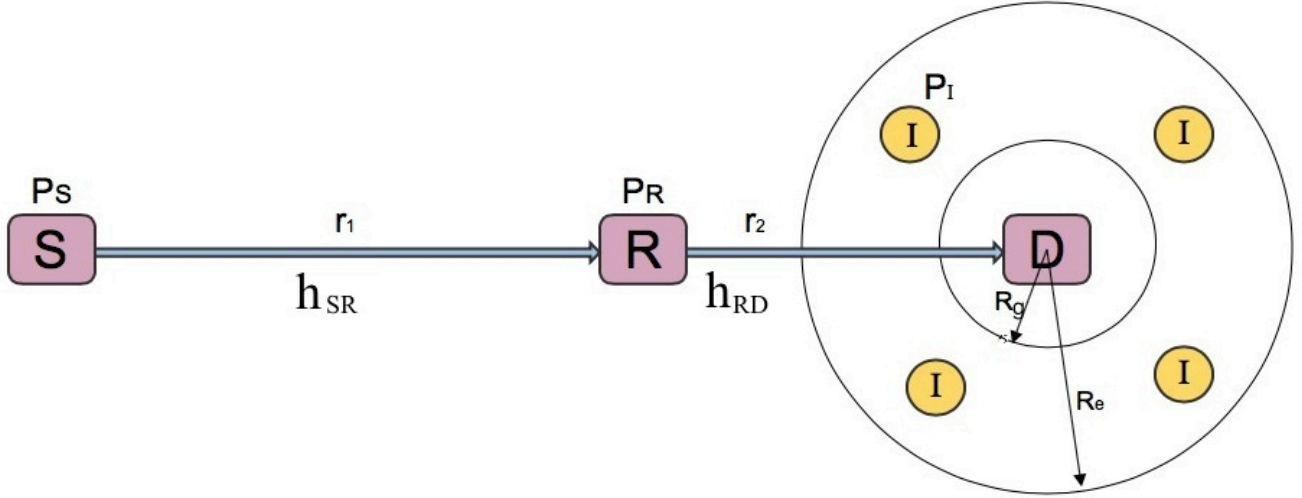
Figure 2.5: Two-hop relay network with Interference at the Destination

Therefore, the end-to-end SINR at the destination can be written as,

$$\gamma_{eq} = \frac{P_S r_1^{-\alpha} |h_{SR}|^2 \left(\dfrac{P_R r_2^{-\alpha}}{P_S r_1^{-\alpha} |h_{SR}|^2 + N_0}\right)^{|h_{RD}|^2}}{\left(\dfrac{P_R r_2^{-\alpha}}{P_S r_1^{-\alpha} |h_{SR}|^2 + N_0}\right)^{|h_{RD}|^2 N_0} + \Sigma P_I r_x^{-\alpha} |h_x|^2},$$

$$\gamma_{eq} = \frac{\left(\dfrac{P_S r_1^{-\alpha} |h_{SR}|^2}{P_S r_1^{-\alpha} |h_{SR}|^2 + N_0}\right) \times \dfrac{P_R r_2^{-\alpha} |h_{RD}|^2}{\Sigma P_I r_x^{-\alpha} |h_x|^2}}{\dfrac{P_R r_2^{-\alpha} |h_{RD}|^2 N_0}{(P_S r_1^{-\alpha} |h_{SR}|^2)(\Sigma P_I r_x^{-\alpha} |h_x|^2)} + 1},$$

23

$$\gamma_{eq} = \frac{\frac{P_S r_1^{-\alpha}|h_{SR}|^2}{N_0} \times \frac{P_R r_2^{-\alpha}|h_{RD}|^2}{\Sigma P_I r_x^{-\alpha}|h_x|^2}}{\frac{P_R r_2^{-\alpha}|h_{RD}|^2}{P_R r_2^{-\alpha}|h_{RD}|^2 N_0} + \frac{P_S r_1^{-\alpha}|h_{SR}|^2}{N_0} + 1},$$

$$\gamma_{eq} = \frac{\gamma_{SR}\gamma_{RD}}{\gamma_{SR} + \gamma_{RD} + 1}.$$

where, $\gamma_{SR} = \frac{P_S r_1^{-\alpha}|h_{SR}|^2}{N_0}$ and $\gamma_{RD} = \frac{P_R r_2^{-\alpha}|h_{RD}|^2}{\Sigma_{x \epsilon \phi} P_I r_x^{-\alpha}|h_x|^2}$. Here, γ_{SR} is the instantaneous signal-to-noise

ratio of S-R channel while γ_{RD} represents the instantaneous signal-to-interference ratio of the R-D channel.

Similar to Section 2.1.1, P$_{out}$ can be written as

$$P_{out} = \boldsymbol{Pr}\left(\frac{\gamma_{SR}\gamma_{RD}}{\gamma_{SR} + \gamma_{RD} + 1} < \gamma_{th}\right).$$

2.2.1 Numerical Results and Discussion

This section presents the outage probability of a two-hop relay networks with interference at the relay for various networks configurations.

Figure 2.6 shows the variation of the outage probability P_{out} with source power P_S for various values of relay power P_R. As P_S increases, P_{out} decreases gradually resulting in better network performance. For example, when $P_R = 2\,W$, an increase of P_S from $2\,W$ to $10\,W$, decreases the outage probability from 1 to 0.68. Further increase of P_S from $10\,W$ to $18\,W$, decreases the outage probability. Therefore, as P_S increases, P_{out} decreases gradually. Considering the plots for $P_R = 2\,W$ and $P_R = 10\,W$, there is a noticeable drop in P_{out}. This drop is due to the Amplify-and-Forward strategy used by the relay, where the relay gain G increases for increase in relay power P_R. However, further increase in relay power shows no dramatic improvement in the outage probability. This is because higher relay gain affects the network performance as it amplifies the interference along with the signal at the relay.
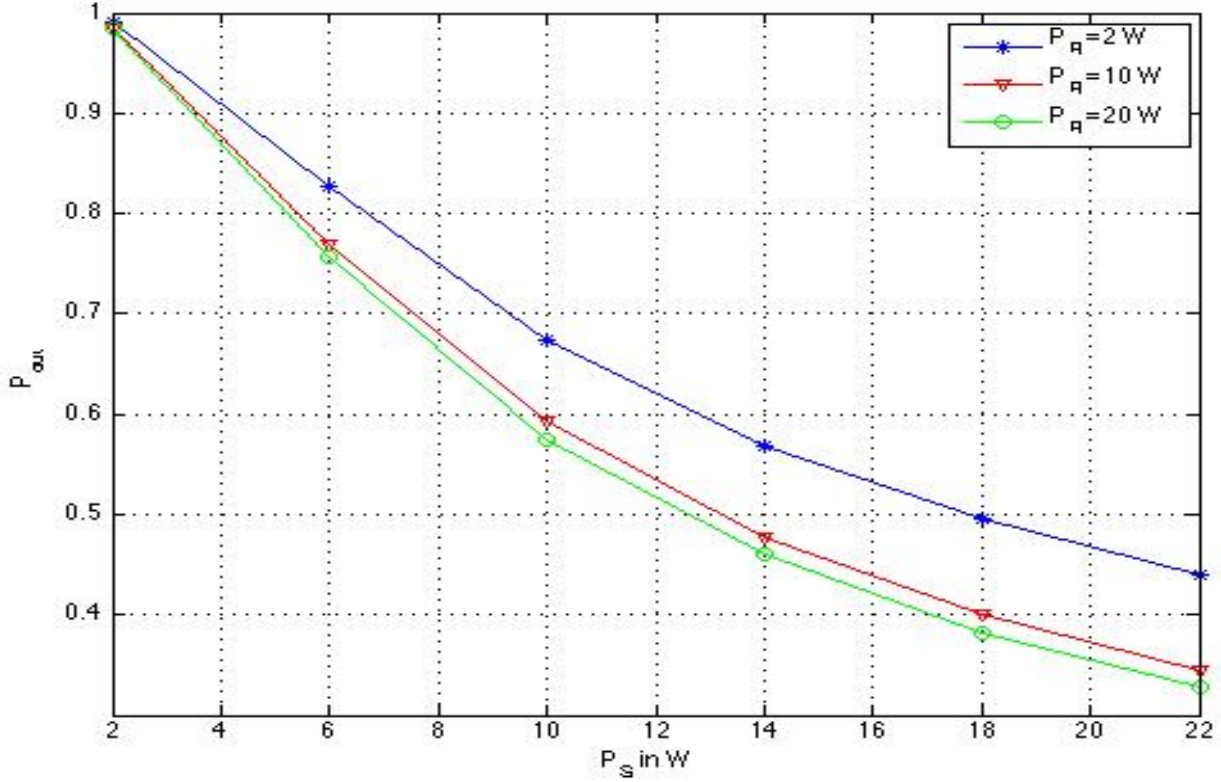
Figure 2.6: Variation of Outage probability with source power P_S for various values of relay power P_R when $\alpha = 3, R_g = 200m, \lambda = 1 \times 10^{-6}, r_1 = 200m, r_1 = 100m.$

The variation of outage probability with the exclusion zone radius R_g for various values of source power P_S is shown in Figure 2.7. R_g defines an exclusion zone for interferers around the destination. This means there are no other base stations, relays, micro cells, pico cells and femto access points are present within R_g. As R_g increases, the outage probability P_{out} decreases which increases the network performance. For example, when $P_S = 30\,W$, an increase of R_g from 0 to $10\,W$ decreases P_{out} from 0.3 to 0.27. This is because the path loss exponentially decays the interference power with its distance to the destination. Therefore, the total interference power at the destination is dominated by the few interferers located in the vicinity of the destination. However, a large increase in R_g is not required as it can reduce the capacity of the network. Defining an exclusion zone at the destination reduces the impact of interference on signal propagation. However, implementing an exclusion zone around the relay is crucial as the relay amplifies the interference along with the signal.
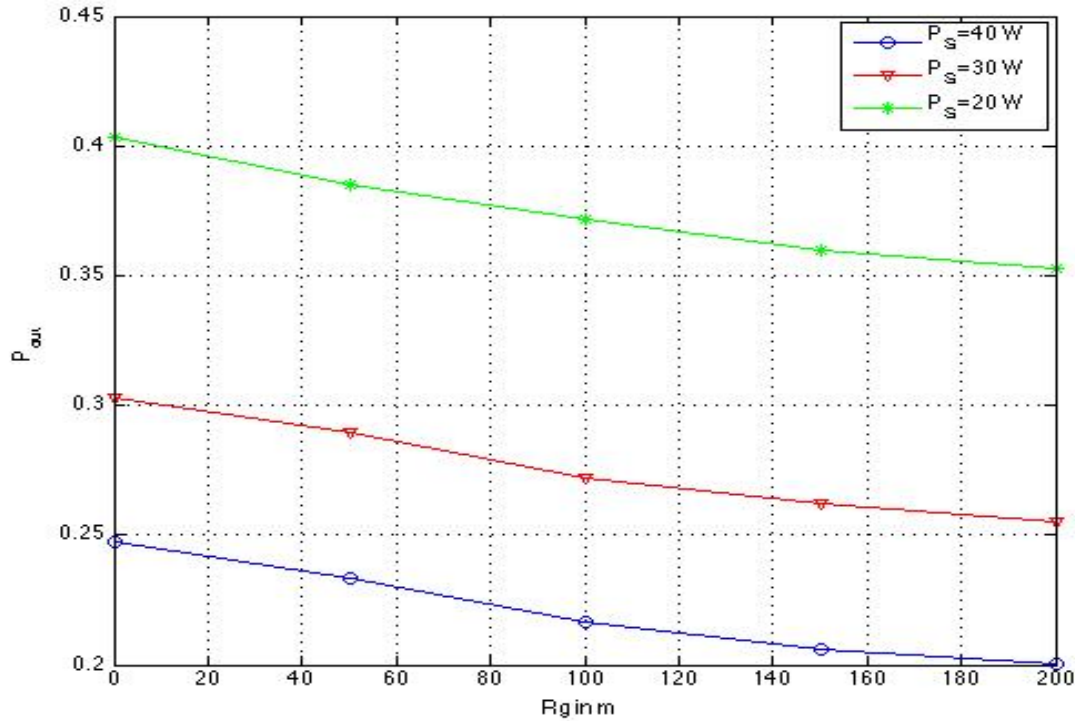
Figure 2.7: Variation of Outage probability with Exclusion zone radius R_g for various of source transmit power P_s when $\alpha = 3, \lambda = 1\times10^{-6}, P_R = 2\,W, r_1 = 200m, r_1 = 100m$.

Figure 2.8 shows the variation of outage probability P_{out} with intensity of interferers λ for various values of source transmit power P_S. The plot shows that the outage probability of the network increases as λ increases. The increase in λ increases the number of interferers residing in the annular region. This increases the total interference at the destination caused by other relays, base stations, micro cells, pico cells and femto access points. Interference degrades the signal quality at the destination, thus reducing the reliability of the network. Consider Figure 2.8, when $P_S = 30\,W,$ an increase of λ from 1 to 5 BSs increases P_{out} from 0.23 to 0.27, thus reducing the performance of the network. Results also show that P_{out} decreases with increase in P_S. Hence the network performance can be improved by increasing the transmitted signal power at the source.
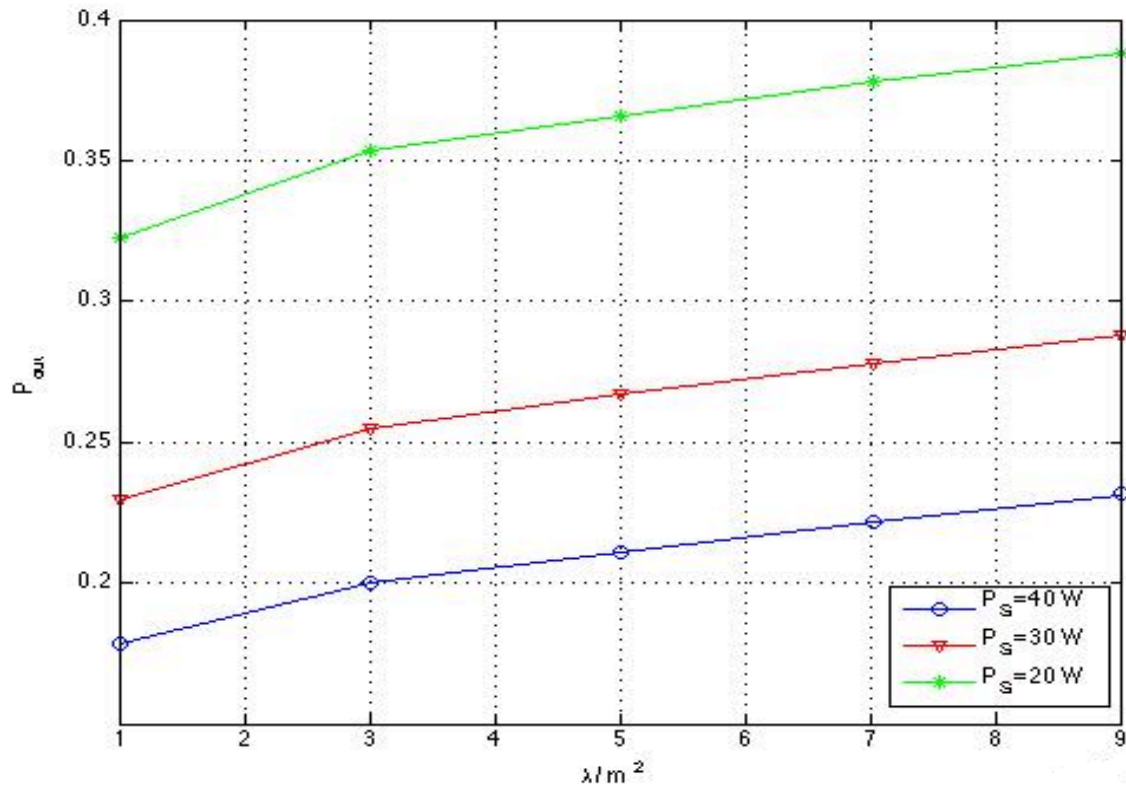
Figure 2.8: Variation of Outage probability with intensity of interferers (λ) for various values of source transmit powers P_S when $\alpha = 3, R_g = 200m, r_1 = 200m, r_2 = 200m$.

2.3 Two Hop relay Network with Interference at Relay and Destination

In this section, both relay and destination are assumed to be under the influence of interference from two independent Poisson field of interferers. The interferers are distributed over annular regions as shown in Figure 2.9. Both source-relay and relay-destination channels are assumed to be interference limited, thus AWGN is ignored. Similar to in Section 2.1, CSI assisted Amplify-and-Forward relaying is assumed.
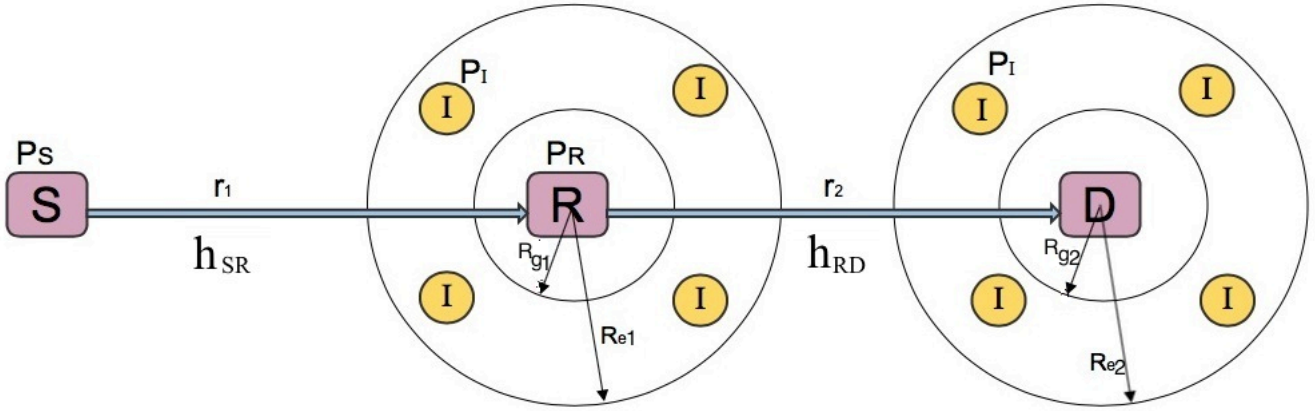
Figure 2.9 Interference at both Relay and Destination

With this configuration, the received signal at the relay can be written as

$$y_R = \sqrt{P_S}\, r_1^{-\frac{\alpha}{2}}\, h_{SR}\, s_0 + \sum_{x \in \Phi} \sqrt{P_{I1}}\, ||x_1||^{-\frac{\alpha}{2}}\, h_{x_1}.$$

Transmit power of interfering nodes $x \in \Phi$ is denoted by P_{I1}. The Euclidean distance between interferer $x \in \Phi$ and the relay is denoted by $||x1||$. Channel gain coefficients are denoted by h_{SR} and h_{x1}. Since CSI assisted variable gain relaying is assumed, the relay amplifies the receive signal by the gain

$$G = \sqrt{\frac{P_R}{P_S r_1^{-\left(\frac{\alpha}{2}\right)} |h_{SR}|^2}}.$$

The received signal at the destination can be written as,

$$y_D = \sqrt{P_R}\, r_2^{-\left(\frac{\alpha}{2}\right)} h_{RD}\, G y_R + \sum_{x \in \varphi} \sqrt{P_{I2}}\, ||x_2||^{-\alpha}\, h_{x_2}.$$

28

The end-to-end signal to interference noise ratio (SINR) at the destination after both phases of communication can be written as

$$\gamma_{eq} = \left[\frac{\Sigma I_1}{P_S r_1^{-\alpha} |h_{SR}|^2} + \frac{\Sigma I_2}{P_R r_2^{-\alpha} |h_{RD}|^2} \right]^{-1},$$

$$\gamma_{eq} = \left[\frac{\gamma_{SR} \gamma_{RD}}{\gamma_{SR} + \gamma_{RD}} \right],$$

where, $\Sigma I_1 = \sum_{x \in \varphi} \sqrt{P_{I1}} \, \|x_1\|^{-\alpha} h_{x_1}$, $\Sigma I_2 = \sum_{x \in \varphi} \sqrt{P_{I2}} \, \|x_2\|^{-\alpha} h_{x_1}$, $\gamma_{SR} = \frac{P_S r_1^{-\alpha} |h_{SR}|^2}{\Sigma I_1}$, and $\gamma_{RD} = \frac{P_R r_2^{-\alpha} |h_{RD}|^2}{\Sigma I_2}$.

Similar to Section 2.1.1, P_{out} can be written as

$$P_{out} = \boldsymbol{Pr} \left(\frac{\gamma_{SR} \gamma_{RD}}{\gamma_{SR} + \gamma_{RD}} < \gamma_{th} \right).$$

2.3.1 Numerical Results and Discussion

Figure 2.10 shows the variation of outage probability P_{out} with relay power P_R for various values of source power P_S. Initially as P_R increases there is a sharp drop in outage probability. However, further increase in relay power, outage probability remains almost constant. Considering Figure 2.10, when $P_S = 10\ W$, an increase of relay power from $2\ W$ to $6\ W$ causes a sharp drop in the outage probability from 0.19 to 0.14. This happens because, in relay networks, the performance is dominated by the performance of the worst hop. However, for further increase in P_R, there is a marginal decrease in outage probability until $P_R = 10\ W$ and remains almost constant thereafter. This is due to the Amplify-and-Forward strategy used at the relay, where the interference is also amplified along with the signal. It can also be seen that an increase in source transmit power of $10\ W$ does not cause much reduction in outage probability. This is due to the transmitted signal undergoing the effect of interference at both relay and destination.
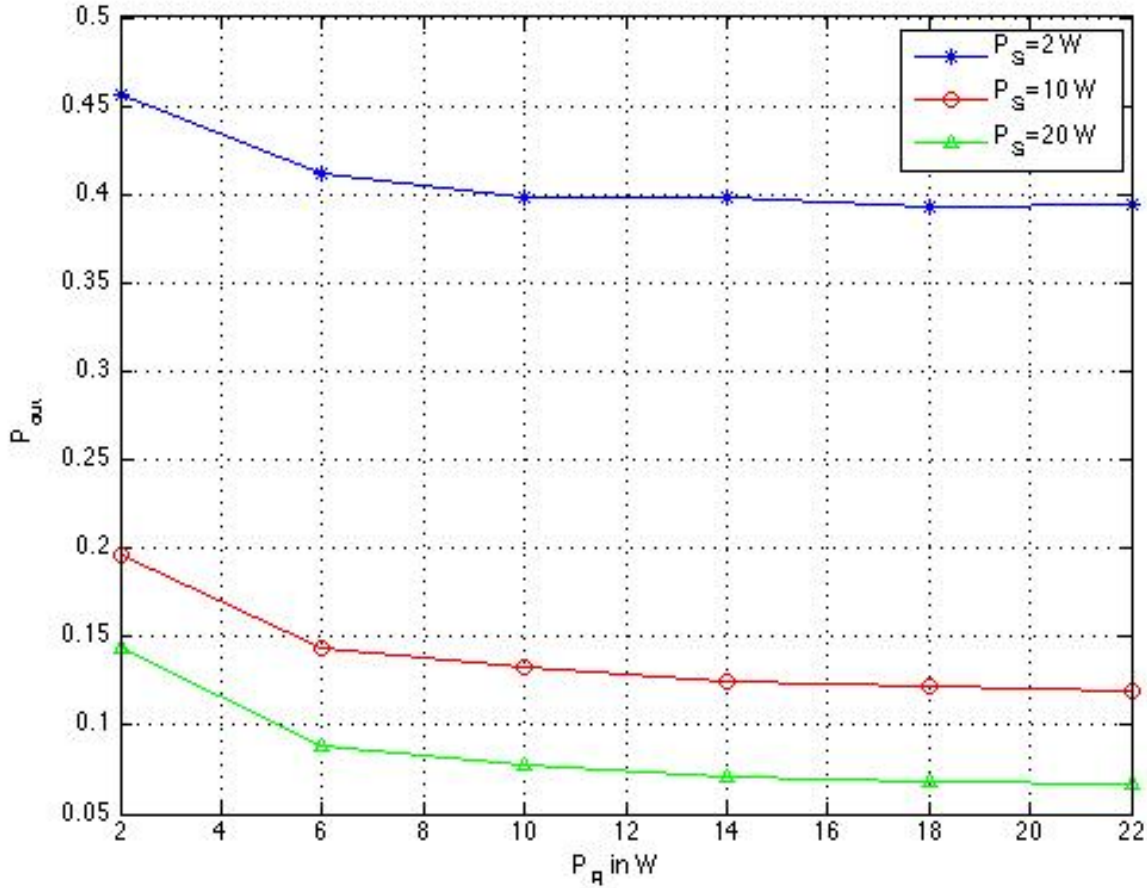
Figure 2.10: Variation of Outage probability P_{out} with relay power P_R for various values of source transmit powers P_S when $\alpha = 3, \lambda = 1 \times 10^{-6}, r_1 = 200m, r_1 = 100m, R_g = 200m$.

The variation of outage probability P_{out} with intensity of interferers λ for various values of relay power P_R is shown in Figure 2.11. From the plot, it can be inferred that the outage probability increases drastically as λ increases. When λ is increased, the total number of interferers in the annular region around the relay and the destination increases. This causes degradation of signal quality and reduces the network reliability. It can also be seen that, a small increase in P_R increases the network performance. However, further increase in P_R causes only a marginal reduction in outage probability. This happens because, higher relay gain detrimentally affects the network performance as at the relay not only the signal it receives but also the interference gets amplified. The degradation of performance of the network is severe when interference is present at relay and destination when compared to interference at relay or destination. This can obviously seen by comparing Figure 2.3 and Figure 2.8 with Figure 2.11.
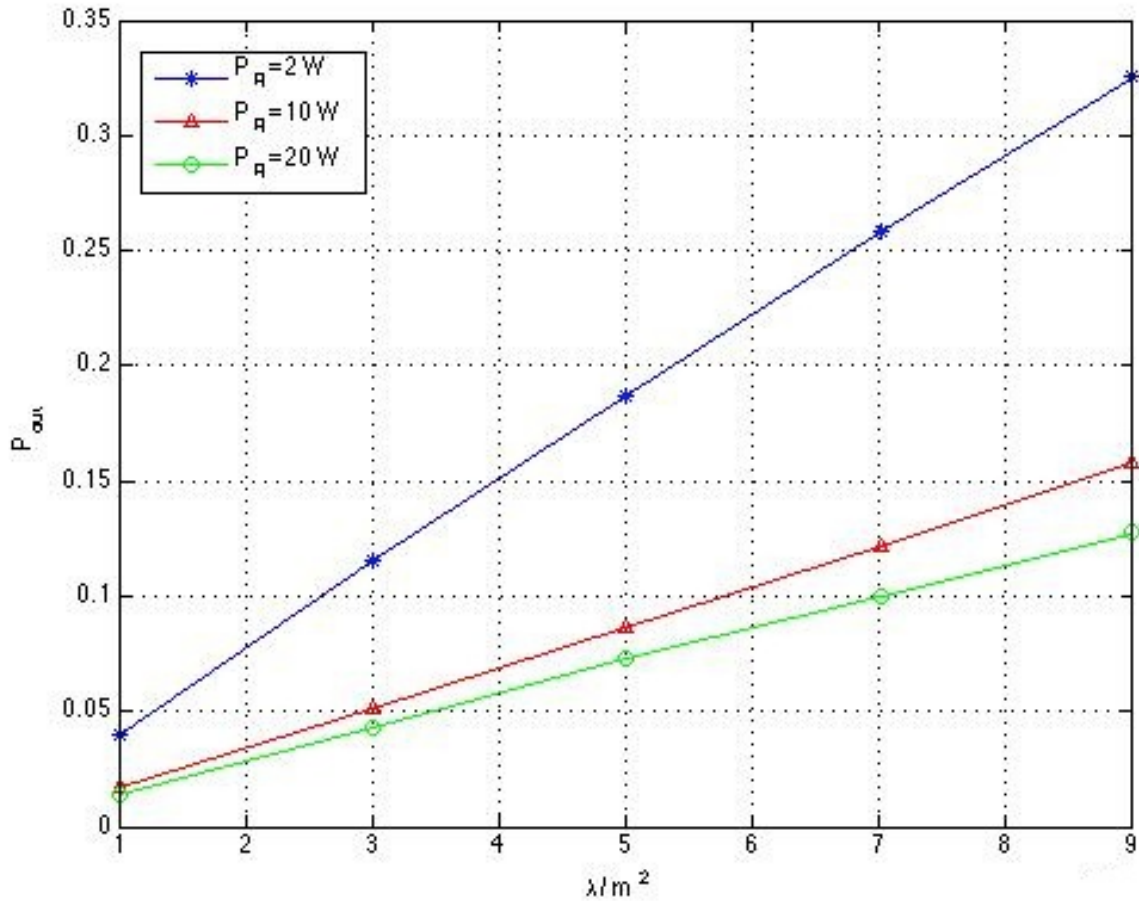
Figure 2.11: Variation of Outage probability P_{out} with intensity of interferers lambda (λ) for various values of relay transmit powers P_R when $\alpha = 3, \lambda = 1 \times 10^{-6}, R_g = 200m, r_1 = 200m, r_1 = 100m$.

Figure 2.12 shows the variation of the outage probability P_{out} with the exclusion zone radius R_g for various values of relay transmit powers P_R. In this case, exclusion zones are considered at both relay and destination. It is assumed that no interferers are located within R_{g1} and R_{g2} (Refer Figure 2.9). Due to this design, the outage probability decreases as R_g increases, resulting in a better network performance. For example, in Figure 2.12, when $P_R = 2\ W$, there is a marginal decrease in P_{out} for an increase in R_g from 0 to 50 m. With further decrease in R_g, there is a constant reduction of outage probability until $R_g = 200\ m$. The network performance is better when exclusion zones are implemented at relay and destination. This can be obviously seen by comparing the drop of outage

31

probability in Figure 2.4 and Figure 2.7 with Figure 2.12. However, as discussed before, increasing the exclusion zone radius R_g to a large extent is not required as it can reduce the capacity of the network.
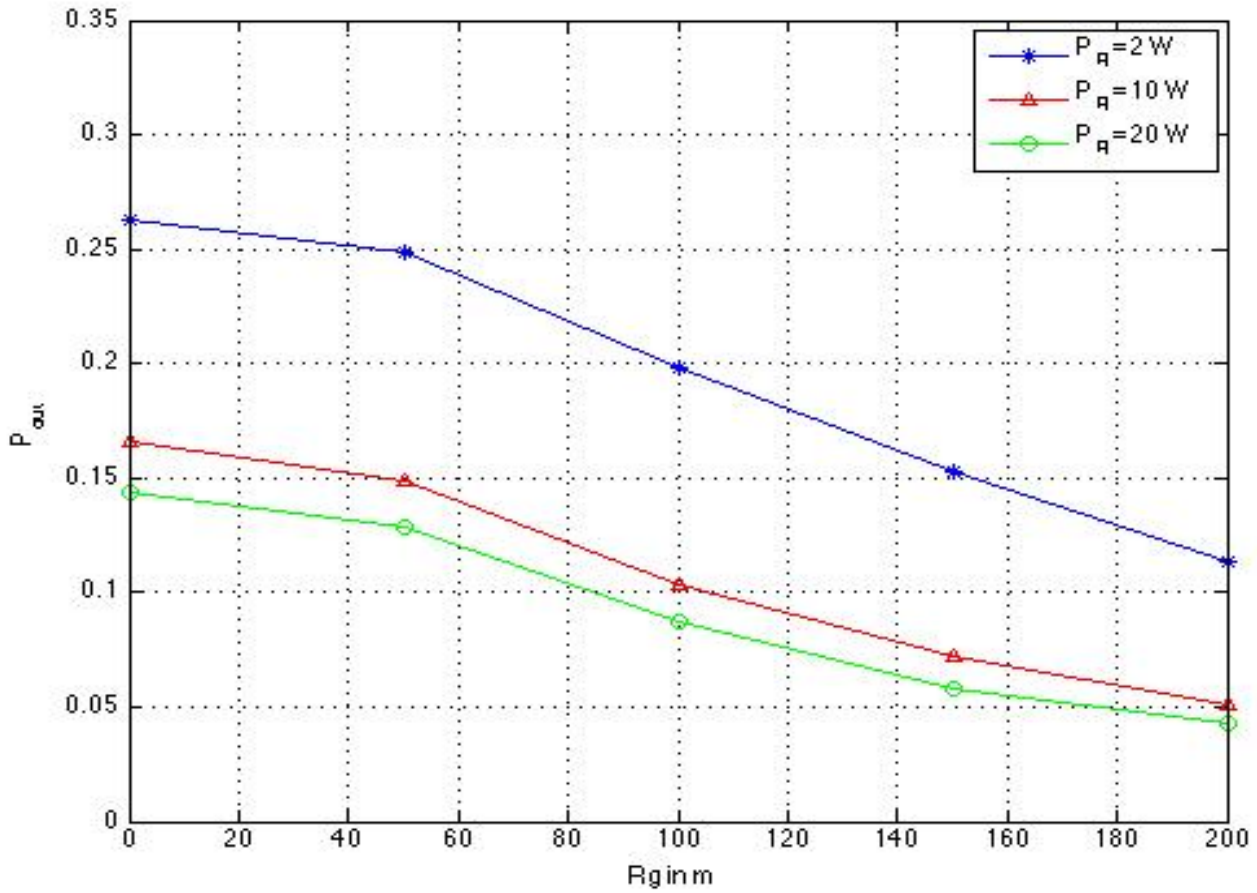

Figure 2.12: Variation of Outage probability P_{out} with Exclusion zone radius R_g for various values of relay transmit powers P_R when $\alpha = 3, \lambda = 1 \times 10^{-6}, r_1 = 200m, r_2 = 100m, P_S = 30\,W$.

Chapter 3

Conclusion

Relay networks have been identified as a promising cost effective solution to meet the demands of ever increasing wireless traffic. However the performance of a relay network can be greatly affected by co-channel interference arises due to aggressive frequency reuse. In this project, the effect of co-channel interference on the outage probability of a two-hop channel state information (CSI) assisted amplify-and-forward (AF) relay network was investigated. The effect of path loss and multipath are considered. The following three cases for the effect of interference on the network were considered.

1. Case I: Relay is subject to interference while the destination is perturbed by additive white Gaussian noise (AWGN).
2. Case II: Relay is under AWGN while destination is subject to interference.
3. Case III: Both relay and destination are subject to interference.

In all three cases, interference at each node was assumed to be generated by a Poisson filed of interferers distributed over an annular region. The effect of having an exclusion zone (inner radius of the annular region), transmit power of the source and the relay, intensity of interferes and path loss exponent were investigate in details.

3.1 Summary and Conclusion

Exclusion zone for interferers: It was found that the effect of interference can be greatly reduced by defining an exclusion zone for interferers around each receiver. It was also found that having a larger exclusion zone is not required due to path loss, which exponentially diminishes the received interference power with the distance. In future generations of wireless networks, path loss will be higher due to the use of higher frequencies and lower antenna heights. Therefore, higher path loss in those networks will ease the effect of interference.

Relay Transmit Power: It was found that relay transmit power increases the outage probability of the network. However, this improvement diminishes as transmit power increases. The reason for this was found to be the amplification of interference at the relay.

Source Transmit Power: Source transmits power was shown to increase the performance of the networks slightly. It was found that this increase in performance diminishes as transmit power increases. This trend was found to be due to the fact that the end-to-end performance of a relay networks is dominated by the performance of the worst hop. When source transmits at a higher power level, the sour-relay hop performs better, however the performance of the network still can be lower due to underperforming relay-destination hop.

Intensity of interferes: Due to increased number of interferers, intensity of interferes was shown to detrimentally affects the outage probability of a relay network. However, it was found that more co-channel users can be allowed when the path loss is higher and by defining exclusion regions.

3.2 Future work

- In this study only the Rayleigh fading and path loss were considered. A natural extension to this work would be to study the performance under more general fading models such as Nakagami-m, Rician, and lognormal shadowing.

- In this study, CSI assisted AF relaying was considered. However, situations can arise in practical networks where the instantaneous CSI of the source-relay channel is unavailable. Therefore, this work can be extended by adapting fixed gain AF relaying.

- This study primarily investigates the effect of co-channel interference on the outage probability of a two-hop AF relay network. It would be interesting to investigate the effect of interference on other performance metrics such as bit error rate, spectral efficiency.

References

[1] J. D. Parsons and J. G. Gardiner, Mobile Communication Systems, New York, NY: Wiley, 1992.

[2] G. L. Stuber, *Principles of Mobile Communication*, 3rd ed. Springer, 2012.

[3] M. Haenggi, J. Andrews, F. Baccelli, O. Dousse, and M. Franceschetti, "Stochastic geometry and random graphs for the analysis and design of wireless networks," *IEEE J. Sel. Areas Commun.*, vol. 27, no. 7, pp. 1029–1046, Sep. 2009.

[4] M. Haenggi and R. K. Ganti, Interference in Large Wireless Networks, *Foundations and Trends in Networking, Vol.* 3, No. 2, 2009.

[5] J. Andrews, "Seven ways that HetNets are a cellular paradigm shift," *IEEE Commun. Mag.*, vol. 51, no. 3, pp. 136–144, Mar. 2013.

[6] M. Haenggi, Stochastic Geometry for Wireless Networks. Cambridge University Press, 2013.

[7] H. Dhillon, R. Ganti, F. Baccelli, and J. Andrews, "Modeling and analysis of K-tier downlink heterogeneous cellular networks," *IEEE J. Sel. Areas Commun.*, vol. 30, no. 3, pp. 550–560, Apr. 2012.

[8] D. Stoyan, W. Kendall, and J. Mecke, Stochastic Geometry and Its Applications, 2nd ed. John Wiley and Sons, 1996.

[9] J. F. C. Kingman, Poisson Processes, Volume 3 of Oxford Studies in Probability. Oxford University Press, New York, 1993.

[10] Andrea Goldsmith, Wireless Communications, Cambridge University Press, 2005.

[11] M. K. Simon and M. S. Alouini, *Digital Communication over fading Channels*. John Wiley, New Jersey, 2005.

[12] J. N. Laneman, *Cooperative Diversity in Wireless Networks: Algorithms and Architectures*. PhD Dissertation, Massachusetts Institute of Technology, Sept. 2002.

[13] Y. Zhao, R. Adve, and T.Lim, "Improving Amplify-and-Forward Relay Networks: Optimal Power Allocation versus Selection," *IEEE Trans. Wireless Commun.*, vol. 6, no. 8, pp. 3118-3123 , Aug 2007.

[14] J. Laneman and G. Wornell, "A Energy-Efficient Antenna Sharing and Realying for Wireless Networks," in Proc.*IEEE Wireless Communications and Networking Conference*, vol.1, pp.7-12, Sep.2000.

[15] R. H. Y Louie, L. Yonghui, H. Suraweera, B. Vucetic, "Peformance Analysis of Beamforming in Two Hop Amplify and Forward Relay Networks with Antenna Correlation," *IEEE Trans. Wireless Commun.*, vol.8, no.6, pp.3132-3141, Jun.2009.

[16] M. O. Hasna and M. S. Alouini, "A Performance Study of Dual-Hop Transmissions With Fixed Gain Relays," *IEEE Trans. Wireless Commun.,* vol.3, no. 6, pp.1963-1968, Nov. 2004.

[17] Y. Fan and J. Thompson, "MIMO Configurations for Relay Channels: Theory and Practice," *IEEE Trans. Wireless Commun.,* vol.6, no. 5,pp. 1774-1786, May 2007.

[18] K. J. Ray Liu, Ahmed K. Sadek, Weifeng Su, and Andres Kwasinski, *Co-operative Communications and Networking.* Cambridge University Press, New York 2009.

List of Abbreviations

AF	Amplify-and-Forward
DF	Decode-and-forward
AWGN	Additive White Gaussian Noise
CSI	Channel State Information
SIR	Signal-to-Interference Ratio
SINR	Signal-to-Interference plus Noise Ratio
PMF	Probability Mass Function
PPP	Poisson Point Process
PDF	Probability Density Function

Appendix

Appendix I: Simulation of Poisson Field of Interferers over an Annular Region

The following Matlab$^{®}$ codes were used to simulate the distribution of Poisson field of interferers over the annular region defined by outer radius R_e and inner radius R_g with intensity λ.

The number of interfering nodes N distributed over the annular region is given by

$$N = poissrnd(\mu)$$

where $\mu = \lambda\pi\,(Re^2 - R_g^2)$ is the mean measure of the PPP over the annular regions. '$poissrnd()$' is the inbuilt Matlab$^{®}$ function to generate values from Poisson distribution.

The $N \times 1$ vector r_{vec} representing the distances from interfering nodes to the relay located at the center of the annular region is given by

$$r_{vec} = sqrt(R_g^2 + (R_e^2 - R_g^2)rand\,(N,1))\,)$$

where '$rand(,)'$ is the Matlab® function to generate values form standard uniformly distribution on the open interval (0,1).